DOI: 10.1002/ejic.200700818

From Interwoven to Noninterpenetration: Crystal Structural Motifs of Two New Manganese–Organic Frameworks Mediated by the Substituted Group of the Bridging Ligand

Zhiyong Fu,*[a] Jianglong Yi,[a] Yuan Chen,[a] Shijun Liao,[a] Ning Guo,[a] Jingcao Dai,*[b] Guodong Yang,[b] Yunxia Lian,[b] and Xintao Wu*[c]

Keywords: Supramolecular frameworks / Crystal engineering / Manganese / Bimetallic units

The respective reactions of the Mn^{II} ion with the homologous ligands 2-aminoterephthalic acid and terephthalic acid afforded two novel manganese–organic compounds, $[Mn(2\text{-}atp)(bipy\text{-}eta)_{0.5}]_n$ (**1**) and $\{[Mn(tp)(bipy\text{-}eta)_{1.5}]\cdot 2H_2O\}_n$ (**2**). These two compounds were characterized by IR spectroscopy, elemental analysis, and single-crystal X-ray diffraction. Compound **1** ($C_{14}H_{11}MnN_2O_4$) belongs to the monoclinic *C2* space group, $Z = 4$ [$a = 11.9355(9)$ Å, $b = 15.522(1)$ Å, $c = 7.9542(6)$ Å, $\beta = 112.591(2)°$], whereas compound **2** ($C_{26}H_{26}MnN_3O_6$) belongs to the monoclinic $P2_1/c$ space group, $Z = 4$ [$a = 10.0330(3)$ Å, $b = 11.9454(1)$ Å, $c = 21.8640(5)$ Å, $\beta = 92.842(2)°$]. Both compounds have bimetallic blocks as basic units. With two bridging carboxylate groups, the Mn···Mn separation in compound **2** is 4.841 Å. By contrast, the distance of the Mn···Mn centers in compound **1** (with the first paddle-like manganese core) is shortened to 3.058 Å by the bridging of four carboxylate groups, which suggests the existence of a Mn–Mn single bond. The paddle-wheel clusters in compound **1** aggregate into a 3D modular framework that interpenetrates in a threefold manner. The binuclear units in **2** extend to a 3D network with a novel bilayer structural motif. The inclusion of the bipy-eta molecules prevents the structure of **2** from being interwoven, and it thus adopts a noninterpenetrating arrangement. The results indicate that variations in the molecular self-assembly are influenced by the substituted group in the bridging ligand.

Introduction

Crystal engineering of metal–organic frameworks has advanced dramatically over the past decade owing to its potential exploitation of functional complexes, such as magnetic, nonlinear optical, microporous, hydrogen storage, and florescent materials.[1] One promising synthetic approach for these materials is the utilization of coordination chemistry to direct the assembly of small building units into an extended macromolecular network.[2] The whole topology of the supramolecular framework can be obtained in different sizes and with different functionalities by modifying the basic units.[3] The coordination sphere in the metal ion and the flexibility of the ligand store the basic geometrical characteristics of the network. Many transition-metal centers such as Cu,[4] Zn,[5] Cd,[6] Co,[7] Ni,[8] and Pt[9] with coordination numbers of four to six have been used to create metal–organic networks with attractive structural topologies. For the connection ligand, the N,N′ donor space flexible ligand 1,2-bis(4-pyridyl)ethane (bipy-eta) can accept the *gauche* and *anti* conformations, which results in the formation of isomers in the coordination polymers,[10] whereas the dicarboxylic acid analogue was proved to be a useful ligand for the construction of mixed-ligand frameworks.[11] In contrast to supramolecular frameworks with mononuclear connected nodes, those containing bimetallic units are relatively unexplored. In recent years, bimetallic units have attracted much attention, as they offer the opportunity to investigate close metal–metal interactions, which are associated with attractive properties.[12] Although many metal–organic networks have been synthesized, the mechanism of their formation is still unclear. Crystal engineering comes to a new stage for understanding the factors that govern the assembly process, which is important for technological development. Solvent,[13] template,[14] and counterion[15] have been revealed as important factors in the self-assembly process. As part of our research interest in the factors affecting supramolecular aggregates, we continued our investigation into the influence of the substituted groups in the bridging ligands.[16] Here, we report our findings on the use of 2-aminoterephthalic acid (2-atp) and terephthalic acid (tp) as connecting units, which differ only in their substituted group.

[a] College of Chemistry, South China University of Technology, Guangzhou, Guangdong 510640, China
Fax: +86-20-87112906
E-mail: zyfu@scut.edu.cn
[b] Institute of Materials Physical Chemistry, Huaqiao University, Quanzhou, Fujian 362021, China
[c] Fujian Institute of Research on the Structure of Matter, Chinese Academy of Sciences, Fuzhou, Fujian 350002, China

Results and Discussion

2-Aminoterephthalic acid and terephalic acid were selected to construct new mixed-ligand coordination polymers with 1,2-bis(4-pyridyl)ethane and the Mn^{II} ion. Structurally, these ligands differ only in that the former contains an amino group, whereas the latter does not. This slight difference can affect the coordination mode of the metal centers, which thus results in various structural motifs. The dicarboxylic acid analogue ligands have many coordination modes, such as chelating bis(bidentate), unidentate, bidentate, chelating bidentate, and so on, depending on the reaction conditions.[17] In this case, the 2-aminoterephthalic acid in compound **1** accepts a bidentate coordination mode, whereas the terephalic acid in compound **2** has a unidentate and bidentate geometry (Scheme 1). In contrast to the loose structure of **1**, the framework in compound **2** displays a compact bilayer structural motif. The reason for this may be due to steric repulsion effects. The existence of the substituted group in the bridging ligand precludes the Mn center to accept high coordination geometry in compound **1**.

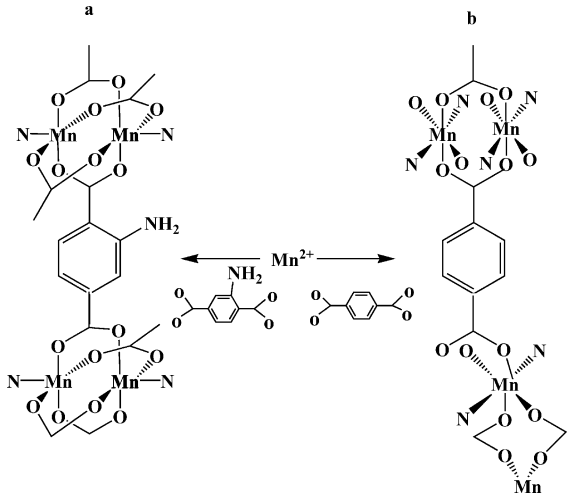

Scheme 1. The coordination modes of the carboxylate groups in compound **1** and **2**: (a) bidentate, (b) unidentate and bidentate.

Crystal Structures

Complexes **1** and **2** were identified by single-crystal X-ray analysis. As illustrated in Figure 1, compound **1** contains a 3D framework with paddle-like binuclear units as the fundamental building blocks. Just as that in the previous Cd,[18] Co,[19] Ru,[20] and Rh[21] paddle-like centrosymmetrical dimers, the Mn metal center here has a distorted square-pyramidal geometry with four O atoms of four 2-aminoterephthalic acid ligands at the equatorial plane and one N atom of 1,2-bis(4-pyridyl)ethane at the apical position. The bond lengths of Mn–O vary from 2.058(14) to 2.111(15) Å. The bond length of Mn–N is 2.163(8) Å (Table 1). These values are similar to those previously reported.[22] The bond angles O–Mn1–O and O–Mn1–N lie in the range 84.2(10)–58.1(7)° and 96.3(7)–05.4(6)°, respectively. The binuclear subunit displays a symmetrical D_{4h} structure, and the Mn atoms have a 16-electron configuration. The Mn···Mn distance between the two manganese centers is 3.058 Å, which indicates the existence of a Mn–Mn single bond.[23] The experimental result is in good agreement with the computed predictions (Mn–Mn 3.00–3.09 Å). The linkage of the Mn centers and the mixed ligands results in a cuboidal structural motif. Eight pairs of manganese bimetallic units occupy the corners, and four long 1,2-bis(4-pyridyl)ethane molecules and eight 2-aminoterephthalic acid ligands make up the 12 edges of the cuboidal box (Figure 2). Aggregation of the cubes forms an α-Po 3D network with 1D channels. The channel width and height are established by the length of 1,2-bis(4-pyridyl)ethane (13.644 Å) and the 2-aminoterephthalic acid (11.075 Å) ligand, respectively (Figure 3). Although large cavities exist in one set of the framework, they are filled by the other two adjacent networks (Figure 4). This is in accord with the fact that a crystal structure with a large cavity is stabilized by the interpenetrating lattices.[24]

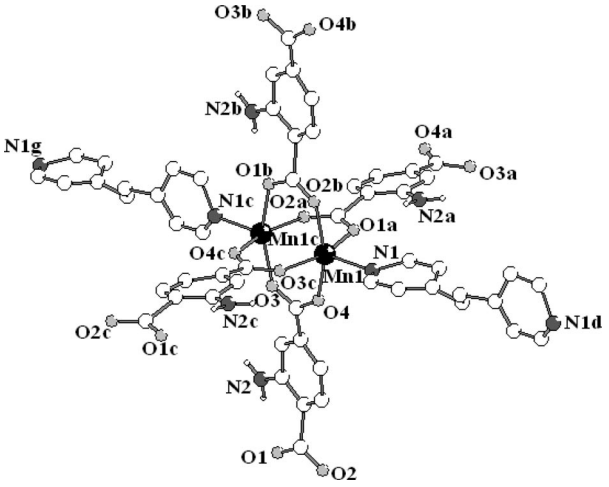

Figure 1. Structure of the paddle-wheel subunit in compound **1**; the hydrogen atoms are omitted for clarity. Symmetry codes: a = $-x + 1/2$, $y - 1/2$, $-z + 2$; b = $x - 1/2$, $y - 1/2$, $z - 1$; c = $-x$, y, $-z + 1$; d = $-x + 1$, y, $-z$; g = $-1 + x$, y, $1 + z$.

Table 1. Selected bond lengths [Å] and bond angles [°] for **1**.[a]

Mn1–O1a	2.058(14)	Mn1–O4	2.111(15)
Mn1–O2b	2.089(17)	Mn1–N1	2.163(8)
Mn1–O3c	2.103(16)		
O1a–Mn1–O2b	84.2(10)	O3c–Mn1–O4	89.8(9)
O1a–Mn1–O3c	158.1(7)	O1a–Mn1–N1	96.3(7)
O2b–Mn1–O3c	87.9(5)	O2b–Mn1–N1	103.2(8)
O1a–Mn1–O4	89.1(6)	O3c–Mn1–N1	105.4(6)
O2b–Mn1–O4	155.6(7)	O4–Mn1–N1	100.8(6)

[a] Symmetry transformations used to generate equivalent atoms for **1**: a = $-x + 1/2$, $y - 1/2$, $-z + 2$; b = $x - 1/2$, $y - 1/2$, $z - 1$; c = $-x$, y, $-z + 1$.

Under the same reaction conditions, the application of terephthalic acid generates another 3D coordination polymer with a novel bilayer structural motif. Just as that in compound **1**, compound **2** is also a mixed-ligand supramolecular framework. X-ray single-crystal analysis revealed

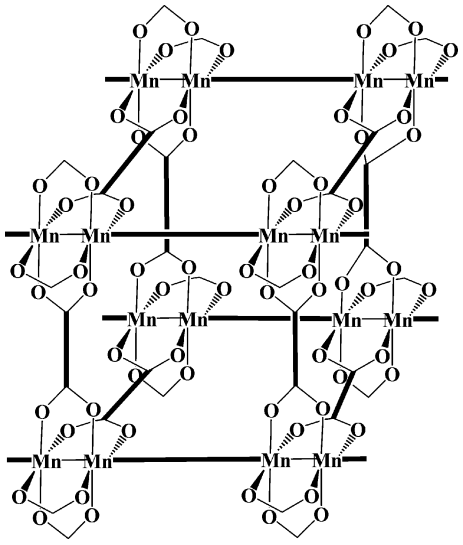

Figure 2. The cuboidal block of **1** showing eight paddle-wheel Mn2 units linked by eight 2-aminoterephthalate and four 1,2-bis(4-pyridyl) ethane rod-like ligands.

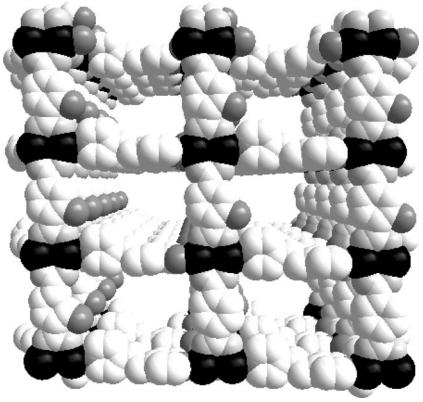

Figure 3. Space-filling model of the regular square cavity in the framework of **1**.

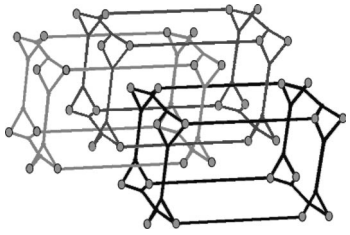

Figure 4. The interpenetration model for complex **1**.

that its structure contains some unique features. The basic unit in the polymer structure is a binuclear block $[Mn_2O_8N_4]$, which lies in a C_2 symmetry geometry (Figure 5). The Mn ion exhibits an octahedral coordination geometry with four oxygen atoms in the equatorial plane (three oxygen donors from the terephthalic acid and one oxygen donor from the coordinated water molecule O5) and two nitrogen atoms at the axial position. The Mn–O distances, which lie in the range 2.136(2)–2.221(2) Å (Table 2), and the Mn–N bond length of 2.261(3)–2.287(3) Å are longer than the values found for compound **1**. The O–Mn–O and O–Mn–N bond angles vary from 83.54(9) to 174.26(9)° and from 86.53(10) to 95.41(10)°, respectively. The N–Mn–N bond angle is 176.77(11)°. These values indicate that the coordination sphere of the Mn metal center adopts a slightly distorted octahedral geometry. The carboxylate arms of the terephthalic acid connect two Mn^{II} ions with a Mn···Mn separation of 4.841 Å, which is longer than that found in compound **1**. Obviously, the paddle-like core in **1** is responsible for this, which has four carboxylate groups between the Mn ions. Figure 6 shows that the connections between the bridging ligand and the Mn ions generate a 4^4 network. The edges of the sheet are constructed by the rods of the linear terephthalic acid ligand, and the binuclear Mn units are located at the corner of the rings. Interestingly, the metal centers, which are distributed in the sheets, are not coplanar. Rather, one falls in a plane,

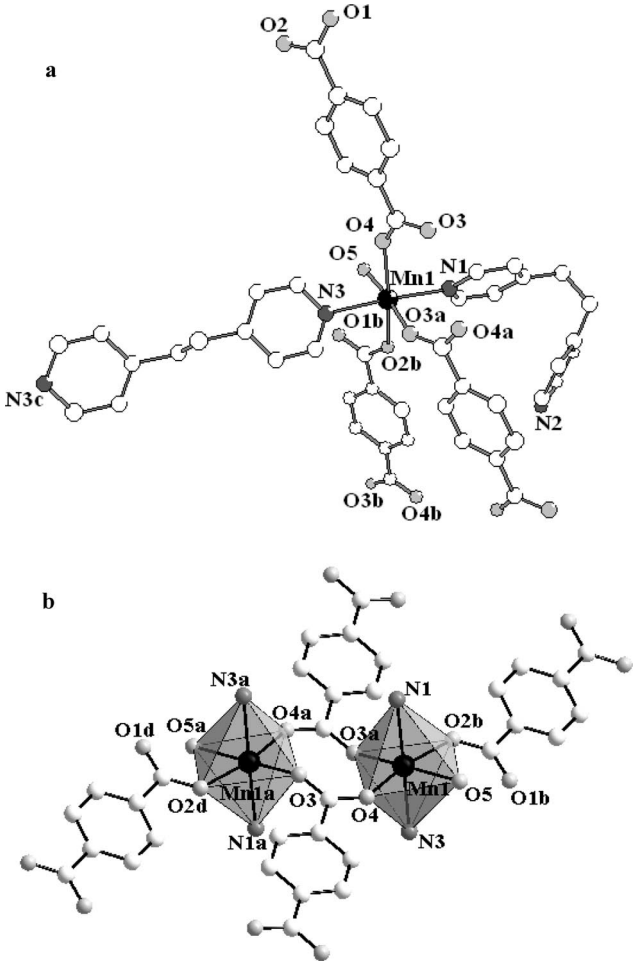

Figure 5. (a) ORTEP drawing of compound **2** around the Mn center; (b) binuclear building block in compound **2**; the hydrogen atoms are omitted for clarity. Symmetry codes: a = –*x*, –*y*, –*z* + 2; b = *x*, –*y* + 1/2, *z* – 1/2.

whereas the other falls in an adjacent plane. This arrangement forms a bilayer structural motif. The connections with the rod-like N,N′ donor spacer ligands 1,2-bis(4-pyridyl)-ethane extend the structural motif to a 3D network with the bilayers as floors (Figure 7). The size of the channel is determined by the length of the mixed ligands (9.26 × 10.97 Å). There are two kinds of 1,2-bis(4-pyridyl)-ethane ligands existing in the frame: one has an *anti* conformation and acts as the pillars of the channel, whereas the other displays a *gauche* conformation and coordinates with the Mn^{II} center as a terminal ligand; it is included into the cavity as a guest molecule. The upper guest 1,2-bis(4-pyridyl)ethane molecule stretches one of its rings into the middle of two lower guest 1,2-bis(4-pyridyl)ethane molecules. The most distinctive structural feature of them can be described as a tongue-and-groove structure, which is a new type of assembly. The guest water molecules are also included in the crystal lattice, and they form a hydrogen bond with the O5 coordinated oxygen atom (O···O = 2.760 Å). Usually, a network with a big cavity adopts an interpenetrating structure mode for the purpose of stability. In this case, the inclusion of the guest molecules prevents the framework from being interwoven; thus, it adopts a noninterpenetrating structure.[25] The host–guest combinations not only help to stabilize the structure, but they also provide a means to manipulate the features of the structure.

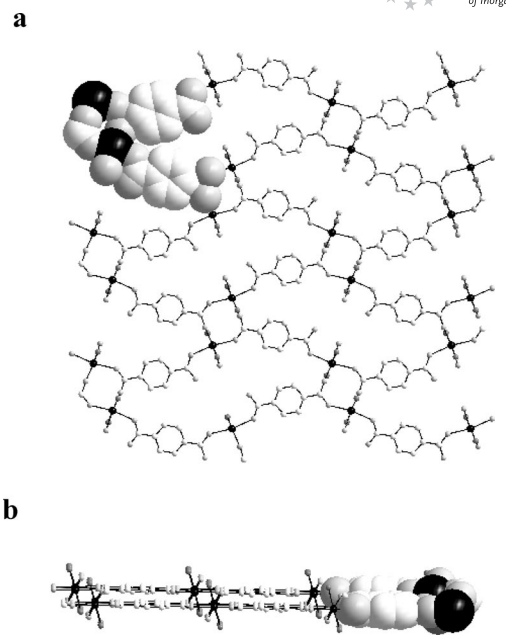

Figure 6. The structure of the bilayer motif: (a) view along the crystallographic *a* axis of the framework; (b) view along the crystallographic *b* axis of the framework.

Table 2. Selected bond lengths [Å] and bond angles [°] for **2**.[a]

Mn1–O3a	2.136(2)	Mn1–O5	2.221(2)
Mn1–O4	2.143(2)	Mn1–N1	2.261(3)
Mn1–O2b	2.189(2)	Mn1–N3	2.287(3)
O3a–Mn1–O4	98.86(9)	O2b–Mn1–N1	87.64(10)
O3a–Mn1–O2b	92.04(9)	O5–Mn1–N1	92.84(10)
O4–Mn1–O2b	168.63(10)	O3a–Mn1–N3	86.53(10)
O3a–Mn1–O5	174.26(9)	O4–Mn1–N3	86.55(10)
O4–Mn1–O5	85.37(9)	O2b–Mn1–N3	90.94(10)
O2b–Mn1–O5	83.54(9)	O5–Mn1–N3	89.88(10)
O3a–Mn1–N1	90.62(10)	N1–Mn1–N3	176.77(11)
O4–Mn1–N1	95.41(10)		

[a] Symmetry transformations used to generate equivalent atoms for **2**: a = –*x*, –*y*, –*z* + 2; b = *x*, –*y* + 1/2, *z* – 1/2; c = –*x* – 1, –*y* + 1, –*z* + 2.

Because π–π interactions play an important role in the self-assembly process,[26] investigation of these contacts may help to understand the formation of the networks in compounds **1** and **2**. Figure 8 shows that the arrangement of two pyridine rings (1 and 2) accepts a typical edge-on T-shaped conformation, which belongs to a C–H···π interaction. The rings (3 and 4) of the 2-aminoterephthalic acid and bipyridine ligands interact and have an off-set stacked geometry.[26] The situation of stacking in compound **2** is similar to that in compound **1**. Two pyridine rings in the bridging ligand and the terminal ligand respectively also have an edge-on T-shaped stacking geometry (Figure 9a), and the π ring planes in the terephthalic acid ligands overlap in a parallel-displaced mode. These weak interactions contribute to the stability of the framework of the structures.

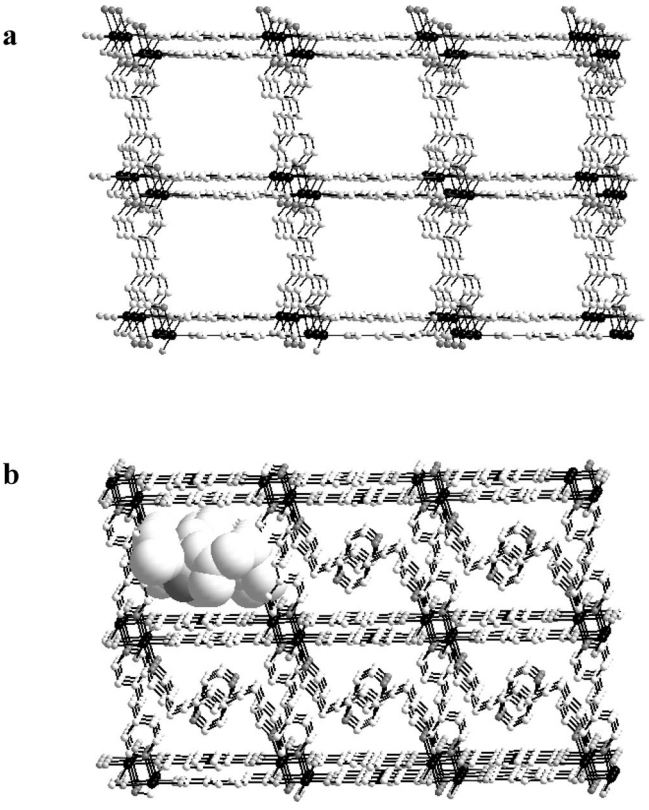

Figure 7. View of the 3D framework in compound **2** (the black spheres indicate the Mn atoms); (a) the open rectangular channels in the framework; (b) inclusion of the large 1,2-bis(4-pyridyl)ethane molecule with *gauche* conformations.

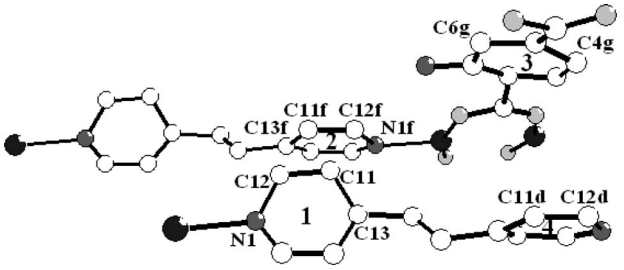

Figure 8. The π–π interactions in compound **1** with the 1,2-bis(4-pyridyl)ethane and the 2-aminoterephthalic acid ligands. Distances [Å]: C11–C12f 2.8166, C11f–C12 2.8166, C11–N1f 3.9623, C12–C13f 3.6238, C4g–C12d 4.0008. Symmetry codes: f = 1 –*x*, *y*, 1 – *z*; g = *x* + 1/2, *y* – 1/2, *z* – 1.

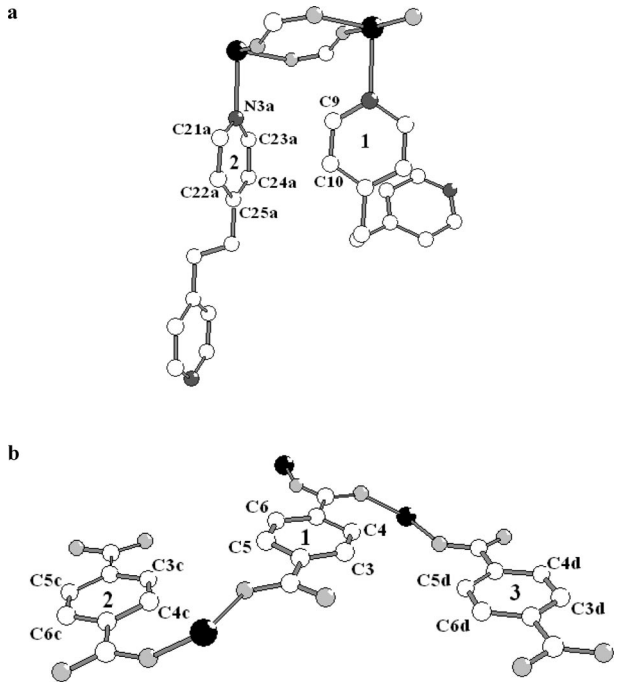

Figure 9. The π–π interactions in compound **2** with the 1,2-bis(4-pyridyl)ethane and the terephthalic acid ligands. Distances [Å]: C9–C21a 3.7631, C9–C23a 3.9566, C10–C22a 3.7098, C10–C24a 3.8522, C4–C5d 3.8507, C3–C5d 3.8516, C5–C4c 3.8507, C5–C3c 3.8516. Symmetry codes: a = –*x*, –*y*, –*z* + 2; c = –*x*, *y* + 1/2, 2.5 – *z*; d = –*x*, *y* – 1/2, 2.5 – *z*.

IR Spectra and Fluorescent Properties

The IR spectrum of compound **1** shows characteristic bands for the dicarboxylate groups of the 2-aminoterephthalate ligands at 1608–1547 cm^{-1} for the asymmetric vibration and at 1456–1429 cm^{-1} for the symmetric vibrations. The IR spectrum of compound **2** shows characteristic bands for the dicarboxylate groups of the terephthalate ligands at 1626–1614 cm^{-1} for the asymmetric vibration and at 1545–1444 cm^{-1} for the symmetric vibration. The absence of the expected characteristic bands at 1730–1690 cm^{-1} that can be attributed to the protonated carboxylate groups indicates the complete deprotonation of 2-aminoterephthalic acid and terephalic acid upon reaction with the Mn ions.[27]

The emission spectra of compounds **1** and **2** in the solid state at room temperature are shown in Figure 8. It can be observed that **1** exhibits intense photoluminescence emission at 410 nm (Figure 10a, λ_{ex} = 310 nm), whereas **2** exhibits intense photoluminescence emission at 427 nm (Figure 10b, λ_{ex} = 315 nm); their emissions may be assigned to ligand-to-metal charge transfer (LMCT).[28]

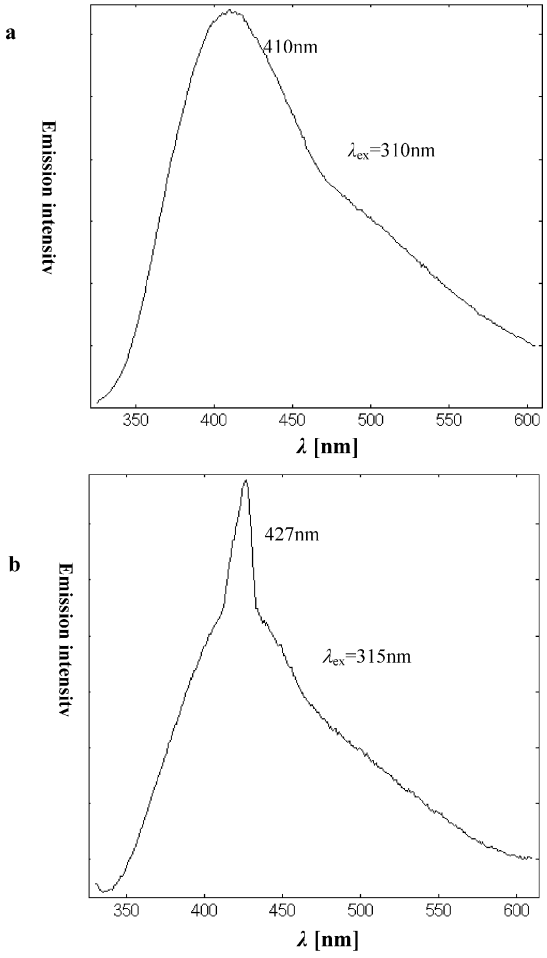

Figure 10. Solid-state emission spectra of the coordination polymers at room temperature: (a) compound **1**; (b) compound **2**.

Conclusions

The effect of the bridging ligands on the structural motifs of coordination polymers was investigated. The experimental results indicate that variations in the molecular self-assembly are influenced by the substituted group in the bridging ligands. The reactions of Mn^{II} ions with the homologous ligands 2-aminoterephthalic acid and terephthalic acid produced two novel manganese–organic compounds, $[Mn(2\text{-atp})(bipy\text{-}eta)_{0.5}]_n$ (**1**) and $\{[Mn(tp)(bipy\text{-}eta)_{1.5}]\cdot 2H_2O\}_n$ (**2**). With the bridging of two carboxylate groups, the Mn···Mn separation in compound **2** is 4.841 Å. In contrast, four bidentate carboxylate groups in the first paddle-like manganese core shorten the Mn···Mn distance to 3.058 Å. This value suggests the existence of a Mn–Mn sin-

gle bond, which is interesting in the research of metal–metal interactions of binuclear structural units. The experimental results support the calculated prediction. Both compounds form 3D frameworks with binuclear $\{Mn_2\}$ units as nodes. The paddle-like framework aggregates into a threefold interpenetrating structural motif, whereas the other extends into a novel bilayer frame resulting in a densely packed network with large guest molecules among them. The inclusion behavior prevents the structure motif of **2** from being interwoven, and instead, it adopts a noninterpenetrating framework. Research on the factors that govern the assembly process is interesting, as it may throw light on the molecular structural design of supramolecular frameworks.

Experimental Section

General: All reactions were carried out under hydrothermal conditions. All chemicals were commercially available and used as received without further purification. The C, H, and N microanalyses were carried out with a Vario EL III elemental analyzer. Infrared spectra (KBr pellets) were recorded in the range from 4000–400 cm^{-1} with a Nicolet Magna 750 FTIR spectrometer. Fluorescent spectra were measured with an Edinburgh FL-FS90 TCSPC system.

$[Mn(2\text{-}atp)(bipy\text{-}eta)_{0.5}]_n$ (1): An aqueous mixture (10 cm^3) containing $MnCl_2{\cdot}4H_2O$ (0.198 g, 1 mmol), 1,2-bis(4-pyridyl)ethane (0.184 g, 1 mmol), 2-aminoterephthalic acid (0.181 g, 1 mmol), and NaOMe(0.108 g, 2 mmol) was placed in a Parr Teflon-lined stainless steel bomb (25 cm^3). The bomb was heated to 160 °C over 27 min. After 24 h at 160 °C, the bomb was cooled to 20 °C at a rate of 0.1 °C min^{-1}, and it was opened to reveal red plate-like crystals (0.17 g, 0.52 mmol, 52% yield). IR (KBr): $\tilde{\nu}$ = 3415 (m), 3188 (m), 3035 (m), 2918 (m), 2850 (m), 1608 (s), 1564 (s), 1547 (s), 1456 (m), 1429 (s), 1365 (s), 1261 (m), 1007 (w), 831 (m), 773 (s), 544 (s) cm^{-1}. $C_{14}H_{11}MnN_2O_4$ (326.19): calcd. C 51.55, H 3.40, N 8.59; found C 51.52, H 3.43, N 8.55.

$\{[Mn(tp)(bipy\text{-}eta)_{1.5}]{\cdot}2H_2O\}_n$ (2): An aqueous mixture (10 cm^3) containing $MnCl_2{\cdot}4H_2O$ (0.198 g, 1 mmol), 1,2-bis(4-pyridyl)-ethane (0.184 g, 1 mmol), terephalic acid (0.166 g, 1 mmol), and NaOMe (0.108 g, 2 mmol) was placed in a Parr Teflon-lined stainless steel bomb (25 cm^3). The bomb was heated to 160 °C over 27 min. After 24 h at 160 °C, the bomb was cooled to 20 °C at a rate of 0.1 °C min^{-1}, and it was opened to reveal colorless block crystals (0.21 g, 0.40 mmol, 59% yield). IR (KBr): $\tilde{\nu}$ = 392 (m), 3238 (m), 3064 (m), 2958 (w), 1626 (s), 1614 (s), 1578 (s), 1545 (s), 1502 (m), 1444 (m), 1385 (s), 1228 (m), 1016 (m), 810 (s), 760 (s), 548 (m) cm^{-1}. $C_{26}H_{26}MnN_3O_6$ (531.44): calcd. C 58.76, H 4.93, N 7.91; found C 58.83, H 4.87, N 7.97.

Crystal-Structure Determination: Crystallographic data for compounds **1** and **2** are listed in Table 3. For compound **1**, a red plate-like crystal with dimensions of $0.24 \times 0.18 \times 0.12$ mm was used. For compound **2**, a colorless crystal with dimensions of $0.34 \times 0.30 \times 0.18$ mm was used. Data for **1** and **2** were collected at room temperature with a Siemens SMART-CCD area-detector diffractometer with Mo-K_α radiation (λ = 0.71073 Å) and graphite monochromator by using the ω scan mode. Data reductions and absorption corrections were performed with SMART and SADABS software, respectively. For all structural analyses, all calculations were performed on an indy workstation of Silicon Graphics with the program SHELXTL.[29] The structures were solved by direct methods. The refinement of structures was performed by full-matrix least-squares techniques on F^2 by using SHELXL97.[30] All non-hydrogen atoms were treated anisotropically. The positions of hydrogen atoms were generated geometrically. Selected bond lengths and bond angles for the cluster cores of **1** and **2** are listed in Tables 2 and 3.

Table 3. Crystal data and structure refinement for **1** and **2**.

	1	**2**
Empirical formula	$C_{14}H_{11}MnN_2O_4$	$C_{26}H_{26}MnN_3O_6$
Formula weight	326.19	531.44
Crystal system	monoclinic	monoclinic
Space group	C2	$P2_1/c$
a [Å]	11.9355(9)	10.0330(3)
b [Å]	15.522(1)	11.9454(1)
c [Å]	7.9542(6)	21.8640(5)
β	112.591(2)	92.842(2)
Volume [$Å^3$]	1360.6 (2)	2617.1(1)
Z	4	4
T [K]	293(2)	293(2)
μ (Mo-K_a) [mm^{-1}]	0.987	0.549
θ range for data collection [°]	2.27 to 25.01	1.87 to 25.05
$d_{calcd.}$ [$g\,cm^{-3}$]	1.592	1.349
F(000)	664	1104
Measured reflections	2141	8922
Independent reflections	1630	4532
Observed reflections[$I > 2\sigma(I)$]	1269	3191
R_{int}	0.0425	0.0374
Goodness of fit on F^2	1.076	1.034
Final R indices [$I > 2\sigma(I)$] R_1, wR_2	0.0786, 0.1609	0.051, 0.1143
R indices (all data) R_1, wR_2	0.1130, 0.1904	0.0855, 0.1320
Largest diff. peak/hole [e $Å^{-3}$]	0.849/–0.778	0.488/–0.386

CCDC-656042 and -656043 contain the supplementary crystallographic data for this paper. These data can be obtained free of charge from The Cambridge Crystallographic Data Centre via www.ccdc.cam.ac.uk/data_request/cif.

Acknowledgments

The authors are grateful for financial support from the Natural Science Foundation of Fujian Province of China (No. 2003F006).

[1] a) C. Janiak, *Dalton Trans.* **2003**, *14*, 2781–2804; b) S. L. James, *Chem. Soc. Rev.* **2003**, *32*, 276–288; c) S.-L. Zheng, X.-M. Chen, *Aust. J. Chem.* **2004**, *57*, 703–712; d) D. Maspoch, D. Ruiz-Molina, J. Veciana, *J. Mater. Chem.* **2004**, *14*, 2713–2723; e) S. R. Batten, K. S. Murray, *Coord. Chem. Rev.* **2003**, *246*, 103–130; f) L. Carlucci, G. Ciani, D. M. Proserpio, *Coord. Chem. Rev.* **2003**, *246*, 247–289; g) M. Dinca, W. Han, Y. Liu, A. Dailly, C. M. Brown, J. R. Long, *Angew. Chem. Int. Ed.* **2007**, *46*, 1419–1422; h) J. Zhang, S. Horike, S. Kitagawa, *Angew. Chem. Int. Ed.* **2007**, *46*, 889–892; i) X. Wang, C. Qin, E. Wang, Z. Su, Y. Li, L. Xu, *Angew. Chem. Int. Ed.* **2006**, *45*, 7411–7414; j) S. Hasegawa, S. Horike, R. Matsuda, S. Furukawa, K. Mochizuki, Y. Kinoshita, S. Kitagawa, *J. Am. Chem. Soc.* **2007**, *129*, 2607–2614; k) M. Dinca, A. Dailly, Y. Liu, C. M. Brown, D. A. Neumann, J. R. Long, *J. Am. Chem. Soc.* **2006**, *128*, 16876–16883.

[2] a) J. Lewinski, M. Dranka, W. Bury, W. Sliwinski, I. Justyniak, J. Lipkowski, *J. Am. Chem. Soc.* **2007**, *129*, 3096–3098; b) J. Zhang, A. Lachgar, *J. Am. Chem. Soc.* **2007**, *129*, 250–251.

[3] a) B. Moulton, M. J. Zaworotko, *Chem. Rev.* **2001**, *101*, 1629–1658; b) . O. R. Evans, W. B. Lin, *Acc. Chem. Res.* **2002**, *35*, 511–522.
[4] X. Zhang, R. Fang, H. Wu, *J. Am. Chem. Soc.* **2005**, *127*, 7670–7671.
[5] X. Lin, A. Blake, C. Wilson, X. Z. Sun, N. R. Champness, M. W. George, P. Hubberstey, R. Mokaya, M. Schroder, *J. Am. Chem. Soc.* **2006**, *128*, 10745–10753.
[6] S. Hasegawa, S. Horike, R. Matsuda, S. Furukawa, K. Mochizuki, Y. Kinoshita, S. Kitagawa, *J. Am. Chem. Soc.* **2007**, *129*, 2607–2614.
[7] Y. Zheng, M. L. Tong, W. Zhang, X. M. Chen, *Angew. Chem. Int. Ed.* **2006**, *45*, 6310–6314.
[8] R. Zou, H. Sakurai, Q. Xu, *Angew. Chem. Int. Ed.* **2006**, *45*, 2542–2546.
[9] W. W. Gerhardt, A. J. Zucchero, C. R. South, U. Bunz, M. Weck, *Chem. Eur. J.* **2007**, *13*, 4467–4474.
[10] T. L. Hennigar, D. C. MacQuarrie, P. Losier, R. D. Rogers, M. J. Zaworoko, *Angew. Chem. Int. Ed. Engl.* **1997**, *36*, 972–973.
[11] a) J. Rowsell, E. Spencer, J. Eckert, J. Howard, O. M. Yaghi, *Science* **2005**, *309*, 1350–1354; b) A. R. Millward, O. M. Yaghi, *J. Am. Chem. Soc.* **2005**, *127*, 17998–17999.
[12] a) G. S. Papaefstathiou, L. d. R. MacGillivray, *Angew. Chem. Int. Ed.* **2002**, *41*, 2070–2073; b) D. N. Dybtsev, H. l. Chun, K. Kim, *Angew. Chem. Int. Ed.* **2004**, *43*, 5033–5036; c) N. L. Toh, M. Nagarathinam, J. J. Vittal, *Angew. Chem. Int. Ed.* **2005**, *44*, 2237 –2241; d) B. Chen, C. Liang, J. Yang, D. S. Contreras, Y. L. Clancy, E. B. Lobkovsky, O. M. Yaghi, S. Dai, *Angew. Chem. Int. Ed.* **2006**, *45*, 1390 –1393; e) C. Zhang, C. Janiak, *Z. Anorg. Allg. Chem.* **2001**, *627*, 1972–1975; f) C. Zhang, C. Janiak, *Acta Crystallogr., Sect. C* **2001**, *57*, 719–720; g) A. Mendiratta, C. C. Cummins, F. A. Cotton, S. A. Ibragimov, C. A. Murillo, D. Villagran, *Inorg. Chem.* **2006**, *45*, 4328–4330; h) F. A. Cotton, A. Yokochi, *Inorg. Chem.* **1997**, *36*, 2461–2462.
[13] R. Robson, B. F. Abrahams, S. R. Batten, R. W. Gable, B. F. Hoskins, J. Liu. *Supramolecular Architecture* (ACS Symposium Series), **1992**, vol. 499, ch. 19.
[14] M. L. Tong, B. H. Ye, J. W. Cai, X. M. Chen, S. W. Ng, *Inorg. Chem.* **1998**, *37*, 2645–2649.
[15] M. A. Withersby, A. J. Blake, N. R. Champness, P. Hubberstey, W. S. Li, M. Schröder, *Angew. Chem. Int. Ed. Engl.* **1997**, *36*, 2327–2329.
[16] Z. Fu, X. Wu, J. Dai, S. Hu, W. Du, H. Zhang, R. Sun, *Eur. J. Inorg. Chem.* **2002**, 2730–2735.
[17] J. C. Dai, X. T. Wu, Z. Y. Fu, C. P. Cui, S. M. Hu, W. X. Du, L. M. Wu, H. H. Zhang, R. Sun, *Inorg. Chem.* **2002**, *41*, 1391–1396.
[18] F. Almeida Paz, Y. Z. Khimyak, A. D. Bond, J. Rocha, J. Klinowski, *Eur. J. Inorg. Chem.* **2002**, 2823–2828.
[19] N. Benbellat, K. S. Gavrilenko, Y. L. Gal, O. Cador, S. Golhen, A. Gouasmia, J. Fabre, L. Ouahab, *Inorg. Chem.* **2006**, *45*, 10440–10442.
[20] W. Z. Chen, F. A. Cotton, N. S. Dalal, C. A. Murillo, C. M. Ramsey, T. Ren, X. P. Wang, *J. Am. Chem. Soc.* **2005**, *127*, 12691–12696.
[21] J. F. Berry, F. A. Cotton, P. L. Huang, C. A. Murillo, X. P. Wang, *Dalton Trans.* **2005**, 3713–3715.
[22] D. Dobrzynska, L. B. Jerzykiewicz, *J. Am. Chem. Soc.* **2004**, *126*, 11118.
[23] Y. Xie, J. H. Jang, R. B. King, H. F. Schaefer, *Inorg. Chem.* **2003**, *42*, 5219–5230.
[24] S. R. Batten, R. Robson, *Angew. Chem. Int. Ed. Engl.* **1998**, *37*, 1460 –1494.
[25] L. Tabares, J. A. R. Navarro, J. M. Salas, *J. Am. Chem. Soc.* **2001**, *123*, 383–387.
[26] C. Janiak, *J. Chem. Soc. Dalton Trans.* **2000**, 3885–3896.
[27] L. J Bellamy, *The Infrared Spectra of Complex Molecules*, Wiley, New York, **1958**.
[28] a) A. Meijerink, G. Blasse, M. Glasbeek, *J. Phys.: Condens. Matter* **1990**, *2*, 6303–6313; b) R. Bertoncello, M. Bettinelli, M. Casarin, A. Gulino, E. Tondello, A. Vittadini, *Inorg. Chem.* **1992**, *31*, 1558–1565; c) J. Tao, M. L. Tong, J. X. Shi, X. M. Chen, S. W. Ng, *Chem. Commun.* **2000**, 2043–2044.
[29] G. M. Sheldrick, *SHELXTL*, Version 5, Siemens Analytical X-ray Instruments Inc., Madison, WI, **1990**.
[30] G. M. Sheldrick, *SHELXL-97: Program for X-ray Crystal Structure Refinement*, University of Göttingen, Göttingen, Germany, **1997**.

Received: August 3, 2007
Published Online: December 3, 2007

